Proceedings of the ASME 2022 Pressure Vessels & Piping Conference
PVP2022
JW Marriott Las Vegas Resort & Spa, Las Vegas, NV, USA

PVP2022-85608

Residual stress modeling and advanced diffraction measurements of 347H steel weldments

Yi Yang[1], Dong Han[1], Yanfei Gao[1]
[1]The University of Tennessee, Knoxville, TN

Wei Zhang[2], Jeffrey R Bunn[2], E Andrew Payzant[2]
[2]Oak Ridge National Laboratory, Oak Ridge, TN

Jorge Penso[3]
[3]Shell Global solution (US) Inc, Houston, TX

Zhili Feng[4]
[4]Oak Ridge National Laboratory, Oak Ridge, TN
Email: fengz@ornl.gov

ABSTRACT

The 347H stainless steel is a primary high-temperature material for many energy and power generation industries. Stress relief cracking (SRC) has been a particular concern in welding of this material. The residual stress induced by welding and its evolution during post-welding heat treatment (PWHT) and subsequent operating and service conditions is one of the primary factors contributing to SRC. The lifetime of welded structure components is also controlled by the precipitation kinetics that accompanies PWHT, stress relaxation process, and long-term aging and complex synergistic factors. Various theories have been proposed in the past to explain SRC. However, a widely accepted approach to predicting the entire damage evolution and the resulting performance reduction is still lacking. This study is to demonstrate a reliable solution for two critical issues that affect the predictions. First, the residual stress distribution obtained from both simulation and neutron diffraction is compared, which increases the accuracy of mechanical analysis simulation model and therefore builds a solid basis for the lifetime prediction model. Second, the generation, evolution, and annihilation of precipitates are monitored by the synchrotron diffraction experiment. Preliminary results demonstrate the critical importance of precipitation kinetics on the residual stress distribution/redistribution during heat treatments.

INTRODUCTION

The 347H austenitic stainless steel has been an excellent material candidate for oil refinery, fossil-fuel power plant, and nuclear plant pipeline systems due to its outstanding creep and corrosion resistance. However, premature failure has become the primary issue that affects the structural integrity and safety. Especially, many recent unexpected cracking issues in the field inspections bring the close attention to the SRC related research. Residual stress can be induced during the welding procedure and its relaxation process proceeds during the PWHT and further aging step (referred to as service time). During the above steps, microcracks may initiate and coalescence at grain boundaries (GBs), and, moreover, accompany with complex microstructural evolution. The welding-induced residual stress/strain level, PWHT conditions, and service environments are all the controlling factors for such convoluted damage and microstructural evolution processes. Thus, an integration of physical metallurgy and mechanics modelling is required to unveil the mechanisms and to develop the mitigation methodologies [1-4].

Residual stress was induced by the intense heat input in the local regime during welding [5]. Fusion zone (FZ) undergoes solidification, whereas heat affected zones (HAZs) usually experience a solutionizing and cooling sequence that generates a microstructure distinctly different from the base metal (BM). Usually, the temperature gradient and the associated thermal expansion and contraction in the above zones are considered to be the root cause for the formation of weld residual stress. However, many previous residual stress prediction models may not give accurate predictions when compared to experimental measurements, and occasionally the predicted values may be off by an order of magnitude [6]. From the viewpoint of material constitutive behavior, most of literature models rely on

the input of the strength versus temperature data, or use laboratory calibrated creep properties. Realistic conditions operate at high temperatures (although with short time span) or intermediate temperature with months to years level time span such as the service condition, so that the material microstructures and defect densities evolve considerably. Accordingly, the continuum constitutive modelling used in residual stress predictions needs to consider the change of plasticity parameters due to the above mentioned evolution processes. An example along this line has been proposed in [7], which suggests the need to incorporate dynamic recovery and dynamic recrystallization in the creep law. In terms of microstructural evolution, it is imperative to quantitatively measure the precipitation kinetics in 347H steels as precipitate is the primary factor for the creep resistance of this material and its evolution critically affects the stress relaxation at elevated temperatures.

In this paper, we present our synergistic modeling/experimental studies on the residual stress development and evolution in 347H steel by a finite element model and neutron and synchrotron X-ray diffraction measurements. Neutron diffraction experiments were performed from which a spatial mapping of the residual stress field can be obtained. Synchrotron X-ray diffraction beam needs to penetrate the sample to obtain the diffraction pattern which limits the thickness of the measurement sample. At the meantime, only spatial mapping can be obtained in the plate plane, due to the cross-section is only 2 mm. Hence, through-thickness information is not available from synchrotron diffraction X-ray measurement. However, precipitation kinetics can be obtained and thus our measurements focus on the correlation amongst residual stress evolution, precipitation, and the ex situ and in situ heat treatment parameters. All these results will provide key inputs for our future failure simulation and lifetime prediction model.

EXPERIMENTAL

Finite element simulation

To compare with the diffraction measurements, finite element simulations have been performed to obtain the residual stress fields upon welding. In order to incorporate the large microstructure gradients across weldments in this study, an integrated microstructure and micromechanical based FEA model was implemented. The 2-dimensional failure model for predicting the failure time was built by using the Voronoi-tessellation method. According to the field inspection report and related literature, the failure in 347H weldments was identified as intergranular creep fracture in the heat affected zone. the mechanisms responsible for the failure process are nucleation of grain boundary (GB) cavities, cavities growth under the competition of GB diffusion and grain interior creep, viscous GB sliding, and these cavities coalescence will cause the microcracks and further will contribute to the final failure. Following this method, the transition of failure mechanisms form creep-controlled to diffusion-controlled creep fracture mechanism can be illustrated. In order to investigate the micromechanical and microstructure origin for 347H weldments failure, finite element methods have been extensively used for this propose [9].

Two simulation steps are listed below.

1. Heat transfer model

A three-dimensional plate was built for generating the temperature field and residual stress distribution/redistribution. Heat source model determines the accuracy of the temperature field distribution, so that the Goldak's double ellipsoid heat source model was applied here. It is not only capable of simulating cases radial symmetry, but also can reduce the computing time without sacrificing accuracy [8]. Hence, Goldak's heat source model has been used for simulating the weldments molten pool widely due to the reliable prediction results.

2. Mechanical analysis

After obtaining the temperature field from heat transfer model, by using the same model setup and adding user subroutine to describe the material mechanical properties, the residual stress field distribution can be obtained. Welding-induced residual stress fields can be easily generated from these two sequential steps. In addition, further heat treatment steps can be added in order to mimic the conditions used in the diffraction measurements. During these heat treatment steps, the entire plate was experiencing the same thermal history, which would cause the residual stress relaxed and redistribution [9-10].

Neutron diffraction

Ex situ neutron diffraction investigation on two plates was conducted at the HIDRA HB-2B beamline, at the High Flux Isotope Reactor (HFIR), Oak Ridge National Laboratory (ORNL). HIDRA is specifically designed for studying the residual stresses in steel, aluminum, superalloys, and structural materials. Elastic strain can be obtained through measuring the interplanar atomic spacing, and, thus, a strain map caused by the applied or residual stress can be obtained through this high penetration power of neutrons. Lab-made welds for neutron diffraction measurements was using commercially purchased 347H plates in dimension of 307.5 mm × 310 mm × 25.4 mm following the same welding procedure that has been typically adopted in petrochemical refinery plants. One plate is in as-welded condition (Sample ID: PWHT 80521-1), another is PWHT at 538℃ for 1 hour then heated to 900℃ and held for 4 hours (Sample ID: PWHT 80521-1), and then removed from the furnace, followed by air cool [11-12].

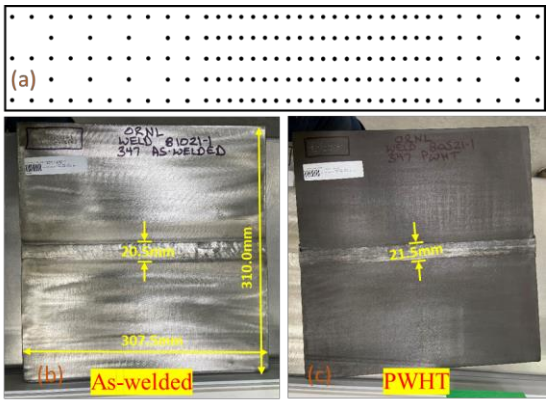

Fig. 1. Neutron diffraction scanning setup: (a) scanning points distributing along the plate cross-section; (b) as-welded plate; (c) after PWHT. (Each plate has dimension of 307 mm × 310 mm × 25.4 mm, as-welded plate has a 20.5 mm weld cap, PWHT plate has a 31.5 weld cap)

Synchrotron diffraction

Ex situ experiments were performed at beamline 11-ID-C, the Advanced Photon Source (APS), Argonne National Laboratory (ANL). A total of 17 samples were cut from a commercially purchased 2mm thick 347H stainless steel sheet, machined into 100 mm × 100 mm × 2 mm small sheets. One sample labeled with As-Received condition means no welding was performed on this sample. One sample with As-Welded condition indicates that only welding was carried out on this sample but without further post-weld heat treatment or deformation. Other 15 samples were welded and then post weld heat treated with detailed PWHT conditions as shown in the Table 1. All PWHT sample were using the same heating and cooling rate which is 10℃/min, and the above heat treatment was conducted at a non-vacuum furnace. All welds and PWHT were made at Materials Joining Group of Oak Ridge National Laboratory.

		Heat treated tempeature			
	temp / time	650℃	800℃	900℃	1100℃
Heat treatment time	None				
	0.5h			900C-0.5h	
	1h			900C-1h	1100C-1h
	2h			900C-2h	
	4h	650C-4h	800C-4h	900C-4h	
	12h	650C-12h	800C-12h		
	24h	650C-24h	800C-24h		
	72h	650C-72h	800C-72h		
	168h	650C-168h	800C-168h		

Table 1. Sample PHWT conditions for ex situ synchrotron diffraction experiments.

Two scanning lines with 43 points per line for each sample was performed for the ex situ measurements as heat treatment was performed prior to the test. One line noted as Mid-row is located at the center of the sheet, where the welding line is perpendicular to the scanning line. Another line noted as Top-row is located at 30 mm away from the Mid-row which is also 20 mm away from the sample edge. Measurement details as shown in Fig. 2. In these samples, BM was approximately starting from 12 mm away from the weld centerline. For the consideration of measuring time, the BM region is scanned from 30 mm away to the HAZ edge which is 30 mm to 12 mm away from weld centerline. a FZ is measured from the sample which has obvious distinction from HAZ, and it has a 6mm width region located in the center. Hence, the HAZs are the region between BM and FZ, which has 9 mm width. The scanning points interval for BM is 2mm, for HAZ and FZ is 1mm.

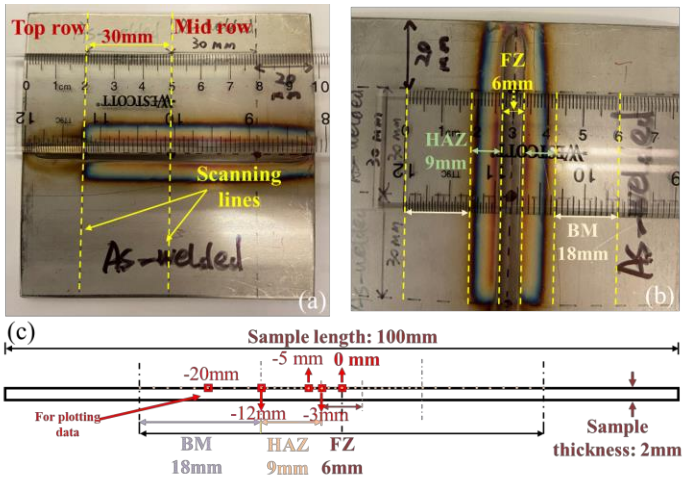

Fig. 2. Sample preparation and setup for ex situ synchrotron diffraction measurements: (a) scanning line positions; (b) regions defined as BM, HAZ, and FZ; (c) scanning point distribution along the cross-section.

RESULTS AND DISCUSSION

1. ABAQUS simulation

Fig. 3 shows the temperature field distribution during the welding process, heat source is moving along the longitudinal direction as the welding pool is presented as the grey area as shown in Fig. 3(a). The temperature gradient caused by the passing heat source in the cross-section is shown in Fig. 3(b) which is able to demonstrate the single pass welding procedure effects on the temperature field distribution. (this simulation setup can make good correlation with our further synchrotron diffraction results which samples was welded by single pass due the thickness limitation induced by the beam penetration capability) From this heat transfer analysis, the thermal histories of each element can be obtained to identify the relationship between temperature and time. The temperature field for the entire plate upon the finish of heat transfer analysis

will be used as the pre-defined field for the calculation of residual stress fields.

Fig. 4 shows the transverse direction residual stress field distribution comparison between as-welded condition and PWHT at 873K situation. The residual stress reduction induced by the PWHT procedure is clearly presented when compare the residual stress contour map of PWHT at 873K and as welded condition contour map as shown in Fig4(a) and (b). The highest residual stress value from approximately 350 MPa in the as welded condition drop to near 110MPa for the PWHT status, which has a more than 200% reduction percentage for this case. The residual stress direction that are responsible for the crack formation is the transverse direction which has nearly three times higher residual stress level than the longitudinal direction. This assumption also has good agreement with currently published literature. As shown in Fig. (c) and (d), which compared the residual stress for both transverse and longitudinal direction at different thickness level. The high residual stress exist in the transverse direction will promote stress concentration sites formation, especially at the grain boundaries and triple junction. The dramatic change of the residual stress value for both TD and LD located at HAZ, hence, the possibility of the microcracks coalesce and propagate will increase, resulting in the HAZ become the most susceptible location for the crack initiation.

Different PWHT temperatures procedure was performed to generate the relationship between degree of residual stress reduction and relative temperature change ($\frac{\Delta T}{T}$). The degree of residual stress reduction was defined as $\Delta\sigma_{res} = \frac{-(\sigma_{PWHT}-\sigma_{As-welded})}{\sigma_{As-welded}}$, and the relative temperature change was defined as $\frac{\Delta T}{T} = \frac{T_{PWHT}-RT}{RT}$. According to Fig. 5, the relationship between $\Delta\sigma_{res}$ and $\frac{\Delta T}{T}$ follows a linear trend. As the PWHT temperature keep increasing, the $\frac{\Delta T}{T}$ is also increasing, the higher temperature change promises a higher residual stress reduction degree.

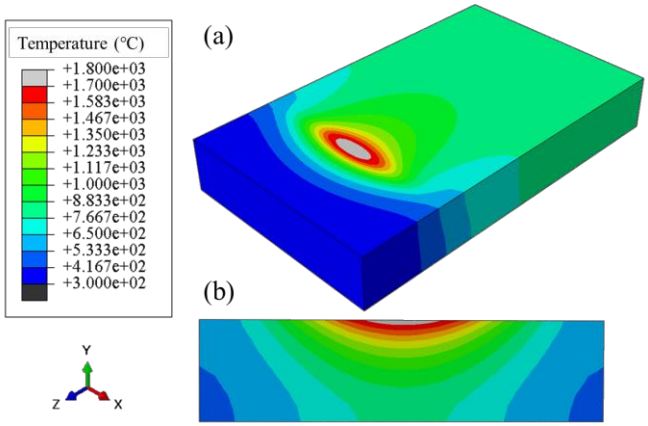

Fig. 3. ABAQUS heat transfer model temperature field distribution: (a) Temperature field distribution during welding process; (b) Temperature gradient along cross-section as the heating source passing through.

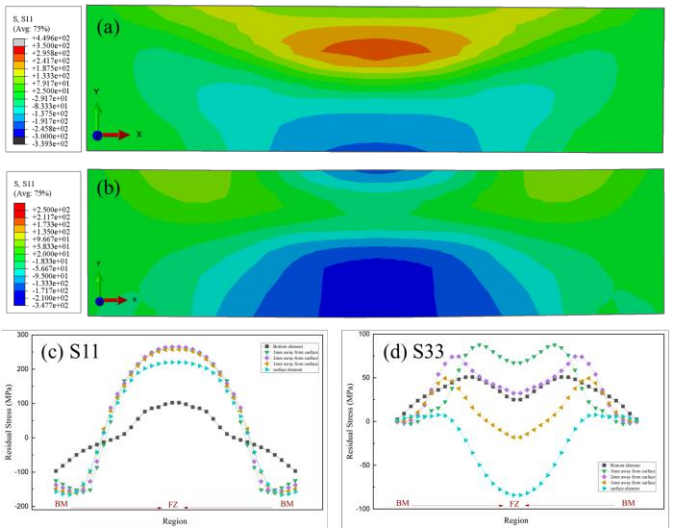

Fig. 4. Simulation results of transverse direction residual stress comparison between (a) As welded condition and (b) PWHT at 873k; (c) Transverse direction (S11) residual stress distribution for the As-welded simulation condition; (d) Longitudinal direction (S33) residual stress distribution for the As-welded simulation condition. All residual stress units in MPa. ($\Delta T = T - RT, T = T_{PWHT}, RT$: $room\ temperature$), unit in ℃.

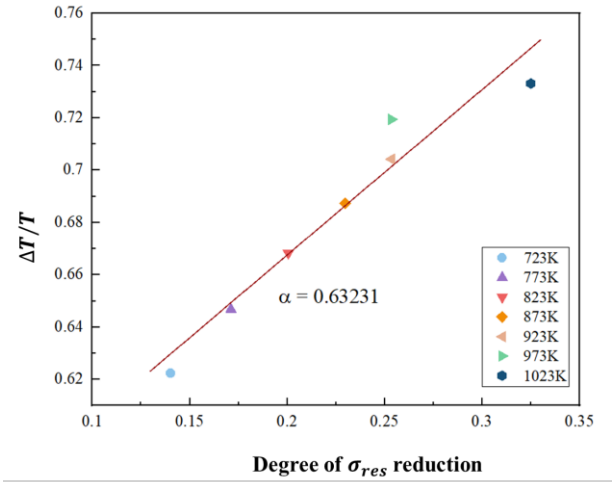

Fig. 5. Relationship between degree of residual stress reduction and relatively temperature change. ($\frac{\Delta T}{T} = \frac{T_{PWHT}-RT}{RT}$ RT: room temperature, units: ℃)

2. Neutron diffraction

The residual stress variation caused by PWHT in the simulation calculation can be validated through neutron diffraction measurement as shown in Fig. 6. As shown in comparison of Fig. 6(a), (b) and (c), (d), it clearly indicates the residual stress gradient around the welding centerline area. As the distance away from the centerline, the residual stress decreases dramatically. The comparison between as-welded condition and PWHT condition, which presented the residual stress reduction effect caused by the PWHT procedure. The plates for the neutron diffraction measurement were produced

by using multi-pass welding procedure, the last pass is not located in the plate center while in the 10 mm away from the weld centerline. The residual stress distribution in the as-welded sample has good agreement with this phenomenon where the highest residual stress is concentrated at the area 10 mm away from the weld centerline. However, in the PWHT plate, the location of the highest residual stress had shift to the center of the plate, accompanied with the residual stress magnitude decrease to approximately 250 MPa compared as-welded condition which is ~500 MPa. The changes occurred above was caused by the PWHT procedure performed on the 'PWHT' plate. The thermal history was followed the same procedure as used in industrial pipeline system for consistency consideration. In Fig. 5(a) and (b), the mainly residual stress component is the tensile residual stress, compressive stress exists in the far end of the plate which may not be detected in the contour map. However, nearly -150 MPa compressive residual stress was measured in the transverse direction for both as-welded and PWHT conditions. This phenomenon was caused by the short term PWHT procedure which is able to relax most of the residual stress induced by the welding process, while the residual stress exists in the fusion zone and HAZ needs long-term thermal treatment due to the microstructure variation happened during the welding process and further thermal treatment.

The accuracy of the simulation model still needs to be improved as the neutron diffraction result can be used as verification data. The current applying boundary condition for the simulation models are lack of ability to fully follow the actual situation, further investigation is still needed to enhance the effect of boundary conditions on residual stress distribution.

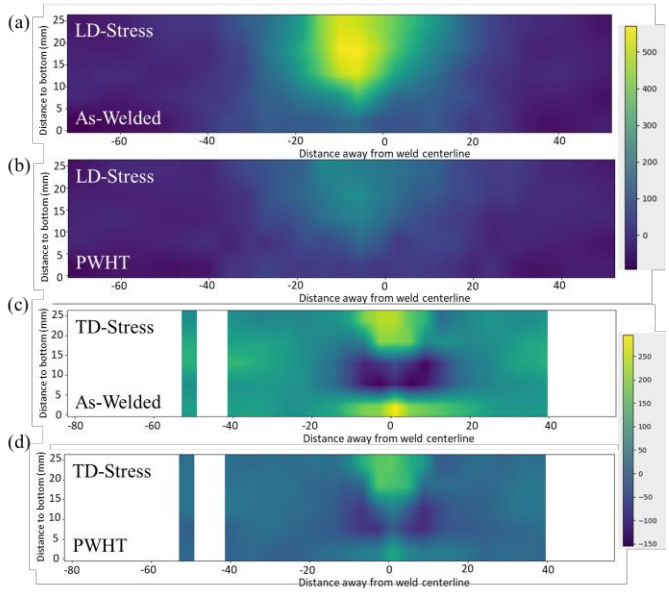

Fig. 6. Neutron diffraction measurement comparison between longitudinal direction and transverse direction residual stress in the As-Welded and PWHT plates. Units in MPa.

3. Synchrotron diffraction

PWHT conditions have a great impact on the residual stress redistribution and precipitation evolution process. Therefore, the study about PWHT condition was conducted by using synchrotron diffraction. As-Welded samples were used as d_0 reference sample in the subsequent calculations, as it is the change of residual stress that matters for this study of PWHT effects.

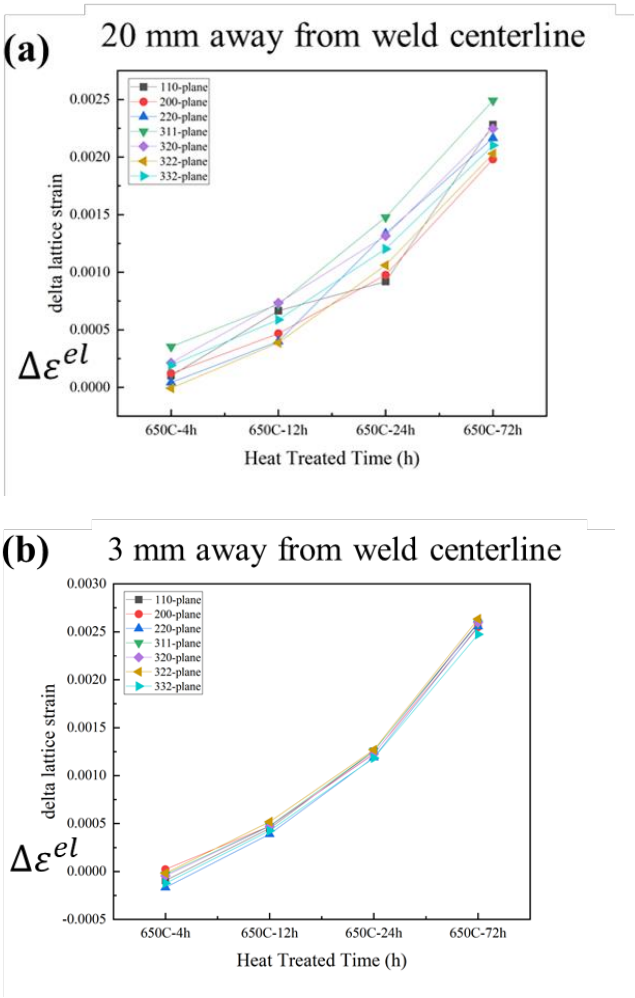

Fig.7. PWHT effect on the change of lattice strain. (a) scanning point 20mm away from weld centerline; (b) scanning point 3mm away from weld centerline.

Equation for calculating the PWHT effect is shown below:

$$\Delta\varepsilon^{el} = \frac{d_{PWHT}^{location\#} - d_{As-Welded}^{location\#}}{d_{As-Welded}^{location\#}} \qquad (1)$$

Fig.7 show the $\Delta\varepsilon^{el}$ variation for samples heat treated at 650°C, as PWHT time increases from 4 hours to 72 hours. It shows a similar trend for the scanning point 20mm, 10 mm, 3 mm, and 0 mm away from the weld centerline. The mechanism of this phenomenon is that the reprecipitating process in HAZ essentially strengthens the material and makes it more creep-resistant. The mismatch among various locations leads to a complex redistribution. Clearly, our finite element simulations need to incorporate such properties in order for an accurate residual stress prediction [14].

Precipitation as the strengthening factor in 347H steels gradually takes control as the heat treatment time increases. The

increasing fraction of MC (metallic carbide, in this case is NbC) enhances the material strength and decreases the creep rate. The HAZ has a negligible amount of precipitates after the welding process due to HAZ's thermal experience is equivalent to a solution annealing, indicating that precipitates in this region are mostly dissolved/annihilated. When PWHT procedure was conducted, those originally annihilated precipitates will re-precipitate into matrix, and, furthermore, these re-generated precipitates can be used as nucleation sites for a higher fraction of precipitates. Further material characterizations are also needed to verify the above reprecipitation process.

CONCLUSIONS

A series of simulation models to evaluate the lifetime of 347H SS weldments are successful to predict the failure time under certain working conditions. The accuracy of the failure model can be verified through neutron and synchrotron diffraction measurements. A synergy of both thermomechanical analysis and microstructural evolution has been built to reveling the undelaying mechanisms of SRC and SAC and making contribution to the lifetime evaluation and the failure location prediction.

Future plan

For further improve the simulation models, three main tasks listed below will be needed to improve the accuracy of the simulation models.

1. Identification of the effect of boundary conditions on residual stress redistribution.
2. Residual stress field measurement on the service pipe to compensates the shape influence on the residual stress distribution
3. Further investigation on the synchrotron diffraction results to explain the effects of precipitates evolution on residual stress field redistribution
4. Integrate all the information above to optimize current failure model for making a more accurate and reliable lifetime prediction model

REFERENCES

1. Z. Wu, J. Penso, T. Chen, D. N. Leonard, D. Zhang, S. A. David, Z. Feng, "Microstructural examination of a 347H austenitic stainless steel weld after 30-years' refinery service", in Proceedings of PVP2020, Minneapolis, Minnesota, 2020.
2. J. Penso, C. Shargay, "Stress Relaxation Cracking of Thick-Wall Stainless Steel Piping in Various Refining Units" in Proceedings of PVP2021, Virtual, 2021.
3. M. E. Fahrion, C. Texaco, A. Birke, J. C. Brown, J. C. Hassell, "Technical basis for improved reliability of 347H stainless steel heavy wall piping in hydrogen service", NACE. Corrosion 2003.
4. C. E. Westhuizen, "Stress relaxation cracking of welded joints in thick sections of a TP 347 stabilized grade of stainless steel", NACE. Corrosion 2008.
5. W. Jiang, K. Yahiaoui, "Effect of welding sequence on residual stress distribution in a multipass welded piping branch junction", International Journal of Pressure Vessels and Piping, vol 95 (2012) 39-47.
6. Z. Feng, X. L. Wang, S. A. David, P. S. Sklad, "Modelling of residual stresses and property distributions in friction stir welds of aluminium alloy 6061-T6", Science and Technology of Welding and Joining, vol 12 (2007), 347-356.
7. X. Yu, P. Crooker, Y. Wang, Z. Feng, "High-Temperature Deformation Constitutive Law for Dissimilar Weld Residual Stress Modeling: Effect of Thermal Load on Strain Hardening", in Proceedings of PVP2015, Boston, Massachusetts, 2015.
8. J. Goldak, A. Chakravarti, M. Bibby, "A New Finite Element Model for Welding Heat Sources", Metallurgical Transactions B, vol 15B (June 1984), 299-305.
9. W. Zhang, X. Wang, Y. Wang, X. Yu, Y. Gao, Z. Feng, "Type IV failure in weldment of creep resistant ferritic alloys: II. Creep fracture and lifetime prediction", Journal of the Mechanics and Physics of Solids, vol 134 (2020), 103775.
10. G. W. Krutz, L. J. Segerlind, "Finite Element Analysis of Welded Structures", Welding Research Supplement, (July 1978), 211-216.
11. C. M. Fancher, J. R. Bunn, J. Bilheux, W. Zhou, R. E. Whitfield, J. M. Borreguero, P. F. Peterson, "pyRS: a user-friendly package for the reduction and analysis of neutron diffraction data measured at the High Intensity Diffractometer for Residual Stress Analysis", Journal of Applied Crystallography, 54, (2021), 1886-1893.
12. P. A. Cornwell, J. R. Bunn, C. M. Fancher, E. A. Payzant, C. R. Hubbard, "Current capabilities of the residual stress diffractometer at the high flux isotope reactor", Review of Scientific Instruments, 89, 9, (2018), 092804.
13. J. G. Nawrocki, J. N. DuPont, C. V. Robino, J. D. Puskar, A. R. Marder, "The Mechanism of Stress-Relief Cracking in a Ferritic Alloy Steel", Welding Research, (Feb 2003), 25-35.
14. B. Shalchi Amirkhiz, S. Xu, J. Liang, C. Bibby, "Creep Properties and TEM Characterization of 347H Stainless Steel", 36th Annual Conference of the Canadian Nuclear Society and 40th Annual CNS/CNA Student Conference, 2016.

ACKNOWLEDGEMENTS

This work was supported by the Shell Projects and Technology team. Neutron diffraction work was carried out at the High Flux Isotope Reactor (HFIR), which is the U.S. Department of Energy (DOE) user facility at the Oak Ridge National Laboratory, sponsored by the Scientific User Facilities

Division, Office of Basic Energy Sciences. The authors thank Dr. Andrey Yakovenko at APS for the technique support. This research also used resources of the Advanced Photon Source; a U.S. Department of Energy (DOE) Office of Science User Facility operated for the DOE Office of Science.

